Journal of the Optical Society of Korea
Vol. 20, No. 1, February 2016, pp. 169-173

ISSN: 1226-4776(Print) / ISSN: 2093-6885(Online)
DOI: http://dx.doi.org/10.3807/JOSK.2016.20.1.169

Investigation on Terahertz Generation by GaP Ridge Waveguide Based on Cascaded Difference Frequency Generation

Zhongyang Li[1]*, Kai Zhong[2], Pibin Bing[1], Sheng Yuan[1], Degang Xu[2], and Jianquan Yao[2]

[1]*North China University of Water Resources and Electric Power, 36, Bei-huan Road, Zhengzhou, Henan 450045, P. R. China*
[2]*College of Precision Instrument and Opto-electronics Engineering, Institute of Laser and Opto-electronics, Tianjin University, Tianjin 300072, P. R. China*

(Received September 7, 2015 : revised November 9, 2015 : accepted February 3, 2016)

Terahertz (THz) generation by a GaP ridge waveguide with a collinear modal phase-matching scheme based on cascaded difference frequency generation (DFG) processes is theoretically analyzed. The cascaded Stokes interaction processes and the cascaded anti-Stokes interaction processes are investigated from coupled wave equations. THz intensities and quantum conversion efficiency are calculated. Compared with non-cascaded DFG processes, THz intensities from 11-order cascaded DFG processes are increased to 5.48. The quantum conversion efficiency of 177.9% in cascaded processes can be realized, exceeding the Manley-Rowe limit.

Keywords : Terahertz wave, Cascaded optical processes, Difference frequency generation
OCIS codes : (190.4410) Nonlinear optics, parametric process; (140.3070) Infrared and far-infrared lasers

I. INTRODUCTION

The terahertz (THz) radiation, which is generally referred to as the frequency from 0.1 to 10 THz, has recently drawn much attention due to its tremendous potential applications, such as imaging, material detection, environmental monitoring, communication, astronomy and national defense security [1-4]. For such applications, a high-power, widely tunable, and compact source of THz-wave is required. Due to the interest in exploiting this region there have been many schemes proposed on source technologies over the last twenty years or so [5-10]. Among many electronic and optical methods for the coherent THz-wave generation, difference frequency generation (DFG) [11-14] is of importance because it offers the advantages of relative compactness, narrow linewidth, wide tuning range, high-power output and room-temperature working environment. In DFG, two optical pump beams, with their frequencies separated by a few THz, interact through a $\chi^{(2)}$ process to generate a THz beam. Unfortunately, the quantum conversion efficiency of the DFG is extremely low as the THz-wave is intensely absorbed by the nonlinear optical crystal. To improve the low quantum conversion efficiency and overcome the Manley-Rowe limit, cascaded DFG in which more than one THz photon is generated from the depletion of a single pump photon is a promising method. Theoretical descriptions and experimental demonstrations of an enhancement output of THz wave via cascaded DFG processes have been reported recently. Liu *et al*. [15] proposed a scheme for monochromatic THz generation via cascading enhanced Cherenkov-type DFG in a sandwich-like waveguide. It is predicted that THz power can be boosted by nearly 8-fold with a 400 MW/cm pump in a 40-mm-long Si-$LiNbO_3$-Si waveguide. Lee *et al*. [16] experimentally observed the fourth-Stokes order in cascaded Stimulated Polariton Scattering utilizing Mg:$LiNbO_3$. Saito *et al*. [17] described a scheme for efficient THz generation using a cascaded optical parametric oscillator using a GaP sheet cavity. By choosing an appropriate pump wavelength and cavity design, the cascading process contributes to efficient THz-wave generation, resulting in a high output peak power of 1.8 MW and a high photon conversion efficiency of 1.086 at 3 THz.

The conversion efficiency of the cascaded DFG process is primarily determined by the effective interaction length

*Corresponding author: thzwave@163.com
Color versions of one or more of the figures in this paper are available online.

and the absorption in the nonlinear optical crystal at THz frequencies. Usually, collinear phase matching is a preferred scheme to maximize the effective interaction length. THz wave generations by GaP rib waveguide via collinear modal phase-matched DFG have been observed [18]. While GaP has a large optical nonlinearity for THz DFG (50 pm/V at 1.55 μm [19]), its absorption coefficient in the THz range is relative large and increases rapidly with increasing frequency. Despite the fact that the THz wave is intensely absorbed by the optical crystal in collinear phase matching configuration, co-propagating the THz wave with the pump and signal waves in the same direction can achieve long- range amplification of the THz wave in a nonlinear crystal until pump depletion [20].

In this paper, we present the theoretical analysis of THz generation by GaP ridge waveguide with a collinear modal phase-matching scheme based on cascaded DFG processes. We investigate the cascaded Stokes interaction processes and the cascaded anti-Stokes interaction processes. THz intensities and quantum conversion efficiency are calculated from coupled wave equations.

II. THEORETICAL MODEL

Figure 1 shows a schematic diagram of THz wave generation by collinear modal phase-matching cascaded DFG. TM-like guided THz wave in the GaP ridge waveguide was generated through type-I phase matching when the electric fields of both pump and signal waves are along $[\bar{1}10]$. THz wave (ω_T) is generated via interactions between the incident pump (ω_p) and signal (ω_s) waves in the first-order DFG process, which consumes the higher frequency pump photon and amplifies the lower frequency signal photon. The amplified signal wave also acts as a higher frequency pump wave, which amplifies the THz wave and generates a new lower frequency cascaded signal (ω_{cs}) wave in the second-order

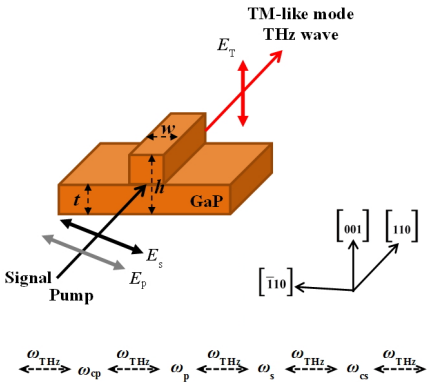

FIG. 1. Schematic diagram of the cascaded DFG to generate THz radiation by GaP ridge waveguide. DFG with Type-I phase matching condition, the electric field vectors of pump and signal wave E_p and E_s are along $[\bar{1}10]$, and that of THz wave E_T is along [001] .

DFG process. Simultaneously, anti-Stokes interactions will also occur that consume the THz photon and pump photon, resulting in a higher frequency anti-Stokes signal (ω_{cp}) wave. The cascaded Stokes processes and anti-Stokes processes can be continued to any high order as long as the phase-matching conditions are satisfied. The intensity of the THz wave is determined by a trade-off between the Stokes processes and the anti-Stokes processes.

THz wave is guided by a GaP ridge waveguide with dimensions t, h, and w, as shown in Fig. 1. Single mode operation of the THz wave produced in the ridge waveguide is realized by satisfying the following condition [21]:

$$\frac{w}{h} < 0.3 + \frac{r}{\sqrt{1-r^2}}, \quad r = \frac{t}{h}, \quad r > 0.5 \tag{1}$$

The collinear modal phase-matching condition in the ridge waveguide is expressed as

$$\frac{n_p}{\lambda_p} - \frac{n_s}{\lambda_s} = \frac{n_{T.eff}}{\lambda_T} \tag{2}$$

where n_i (i=p, s and $T.eff$) correspond to the refractive index of the pump, signal and the TM-like guided THz wave, respectively. λ_i (i=p, s and T) correspond to the wavelength of the pump, signal and the TM-like guided THz wave, respectively. The mode effective index $n_{T.eff}$ of the THz wave is calculated using the effective-index method [22].

The coupled wave equations of cascaded DFG can be derived from common nonlinear optical three-wave interaction equations, shown as

$$\frac{dE_T}{dz} = -\frac{\alpha_T}{2}E_T + \kappa_T \sum_1^{+\infty} E_n E_{n+1} cos(\Delta k_n z) \tag{3}$$

$$\frac{dE_n}{dz} = -\frac{\alpha_n}{2}E_n + \kappa_n E_{n-1} E_T cos(\Delta k_{n-1} z) - \kappa_n E_{n+1} E_T cos(\Delta k_n z) \tag{4}$$

$$\kappa_n = \frac{\omega_n d_{eff}}{c n_n} \tag{5}$$

$$\kappa_T = \frac{\omega_T d_{eff}}{c n_{T.eff}} \tag{6}$$

$$\Delta k_n = k_n - k_{n+1} - k_T \tag{7}$$

$$\omega_T = \omega_n - \omega_{n-1} \tag{8}$$

$$I = \frac{1}{2} n_n c \varepsilon_0 |E|^2 \tag{9}$$

where ω_n and ω_T denote the frequency of pump and THz wave, respectively. E_n and E_T denote the electric field

amplitude of pump and THz wave, respectively. α_n and α_T denote the absorption coefficient of pump and THz wave in the optical crystal, respectively. Δk_n indicates the wave vector mismatch in the cascaded DFG process, κ_n and κ_T are the coupling coefficients. d_{eff} is the effective nonlinear coefficient, and the d_{eff} is 50 pm/V at 1.55 μm [19]. c is the speed of light in vacuum, ε_0 is the vacuum dielectric constant, I is the power density, n_n is the refractive index. The generation and consumption of THz photons are accomplished during the interaction between the n-order and (n+1)-order Stokes waves, as shown in Eq. (3). The second item in the right side of the equal sign in Eq. (4) shows the Stokes processes where THz photons and n-order Stokes photons are generated, and the third item in the right side of the equal sign in Eq. (4) shows the anti-Stokes processes where THz photons and (n+1)-order Stokes photons are consumed.

The theoretical values of refractive index are calculated using a wavelength-independent Sellmeier equation for GaP in the IR [23] and THz [24] range, respectively. The Sellmeier equation for GaP of Madarasz *et al.* [23] in the IR range can be written as

$$n^2(\lambda) = 1 + \frac{1.390\lambda^2}{\lambda^2-0.172^2} + \frac{4.131\lambda^2}{\lambda^2-0.234^2} + \frac{2.570\lambda^2}{\lambda^2-0.345^2} + \frac{2.056\lambda^2}{\lambda^2-27.52^2} \quad (10)$$

The Sellmeier equation for GaP in the THz range [24] can be written as

$$(n+i\kappa)^2 = \varepsilon(\nu) = \varepsilon_\infty + \frac{\rho\nu_{TO}^2}{\nu_{TO}^2-\nu^2-i\gamma\nu} \quad (11)$$

where $\varepsilon(\nu)$ is the complex dielectric constant, ν is the wave-number, ε_∞ is the high-frequency dielectric constant, ν_{TO}, ρ and γ are the eigenfrequency, oscillator strength and damping coefficient of the 367 cm^{-1} polariton mode in GaP, and $\varepsilon_\infty = 9.07$, $\rho = 1.945$, $\nu_{TO} = 367$ cm^{-1}, $\gamma = 9.0$ cm^{-1}.

III. CALCULATIONS

Here, in simulating the cascaded DFG dynamics, pump wave ω_p and signal wave ω_s are supposed to be 193.55 and 192.55 THz, respectively. THz frequency ω_T is taken to be 1 THz. We set the dimensions of GaP ridge waveguide t, h, and w to 120, 200 and 80 μm, respectively. The mode effective index $n_{T,eff}$ for 1 THz is 3.1405 to realize collinear modal phase-matching DFG in GaP ridge waveguide. The wave vector mismatch Δk and coherence length in cascaded DFG processes is shown in Fig. 2. In the cascaded Stokes processes, wave vector mismatch is less than 3.14 cm^{-1} during 11-order cascaded processes. In the case of cascaded anti-Stokes processes, wave vector mismatch is less than 3.14 cm^{-1} during 10-order cascaded processes. In the following calculations, 11-order cascaded Stokes and 10-order cascaded anti-Stokes processes are taken into account as the coherence length is larger than 1 cm. As shown in Fig. 3, THz intensities in GaP ridge waveguide based on cascaded DFG with cascading orders 1, 3, 5, 10 and 11 versus crystal length are calculated according to Eqs. (3) and (4). The intensity of both pump and signal wave are 20 MW/mm^2. The absorption coefficient at 1 THz is 2.5 cm^{-1}[25]. From Fig. 3 we find that THz intensities without cascading processes are extremely low. THz intensities with cascading order 3, 5, 10 and 11 are enhanced. THz intensity of 0.37 MW/mm^2 can be obtained with 11-order cascaded Stokes processes. Compared with non-cascaded DFG processes, THz intensities from 11-order cascaded DFG processes are increased to 5.48. In non-cascaded DFG processes, at best, a single THz photon is generated from each pump photon. The cascaded processes can enhance the THz output, simply by generating several THz photons from each pump photon.

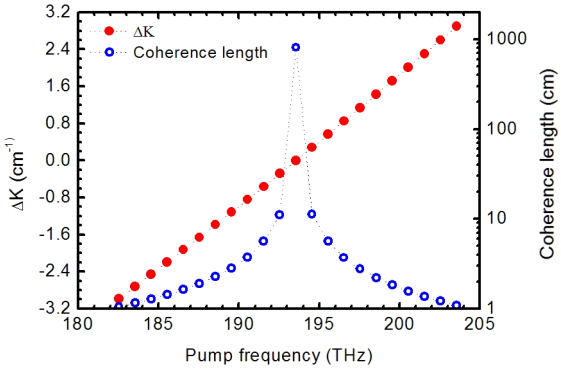

FIG. 2. Wave vector mismatch and coherence length of cascaded DFG. Assuming ω_p =193.55 THz, ω_s =192.55 THz, ω_T = 1 THz.

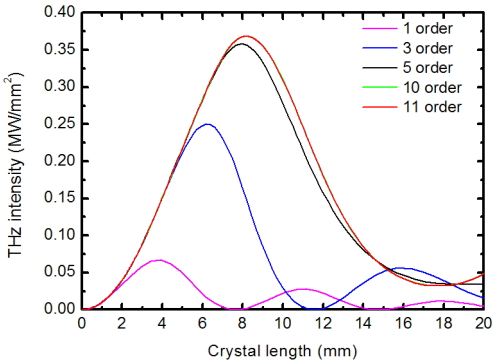

FIG. 3. THz intensities by GaP ridge waveguide based on cascaded DFG with cascading orders 1, 3, 5, 10 and 11.

As the Stokes processes generate THz photons and the anti-Stokes processes consume THz photons, THz intensities depend on the Stokes processes and the anti-Stokes processes. Figure 4 shows the maximum intensities of the optical waves during the cascaded Stokes processes and anti-Stokes

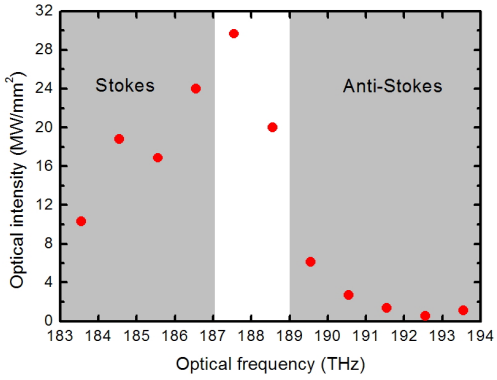

FIG. 4. The maximum intensity of the optical waves during the cascaded Stokes processes and anti-Stokes processes. Assuming the initial pump and signal waves are 188.55 and 187.55 THz with a power density of 20 MW/mm^2, respectively.

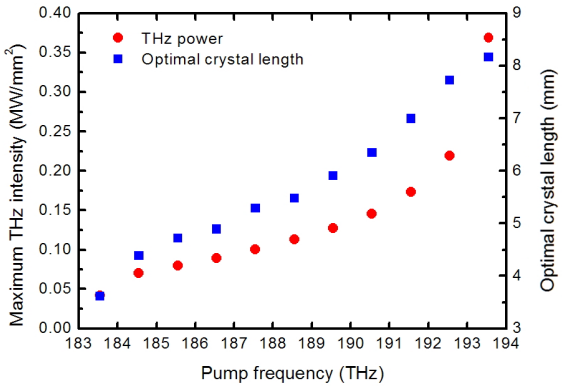

FIG. 5. The relationship between the maximum THz intensities and pump frequencies. Both the pump and signal intensities are 20 MW/mm^2.

processes. In this figure we assume that the optical waves at interval of 1 THz with frequencies from 183.55 to 193.55 THz interact in the Stokes and anti-Stokes processes. The initial pump and signal waves are 188.55 and 187.55 THz, respectively, with a power density of 20 MW/mm^2. From the figure we find that the power densities of optical waves in the Stokes processes is higher than that of optical waves in the anti-Stokes processes, which indicates that the Stokes processes are stronger than the anti-Stokes processes. In the cascaded Stokes processes, n-order Stokes photons are consumed and (n+1)-order Stokes and THz photons are amplified. The cascaded Stokes processes continue to amplify the (n+1)-order Stokes and THz photons as long as the phase-matching conditions are satisfied. Actually, the anti-Stokes processes take place only if the Stokes processes generate THz photons. The anti-Stokes processes consume high-order Stokes and THz photons, and the processes will stop if the high-order Stokes and THz photons are exhausted.

Figure 5 shows the relationship between the maximum THz intensities and the pump wave frequencies. In this figure we assume that the optical waves at interval of 1 THz with frequencies from 183.55 to 193.55 THz interact in the cascaded Stokes and anti-Stokes processes. The frequency of the pump wave is 1 THz larger than that of the signal wave. Both the pump and signal intensities are 20 MW/mm^2. From the figure we find that THz intensities are higher as the pump frequencies locate in the high-frequency area. The high THz intensities originate from the interaction of the high-order Stokes processes as the pump frequencies locate in the high-frequency area, which indicates that the Stokes processes are stronger than the anti-Stokes processes. As the pump frequency equals 193.55 THz, THz wave with a maximum intensity of 0.3686 MW/mm^2 can be obtained. In the high-frequency area where high-order Stokes processes interact, optimal crystal lengths are longer considering cascading, which is consistent with the principle of cascaded nonlinear processes.

Pump intensity is directly related to the quantum conversion

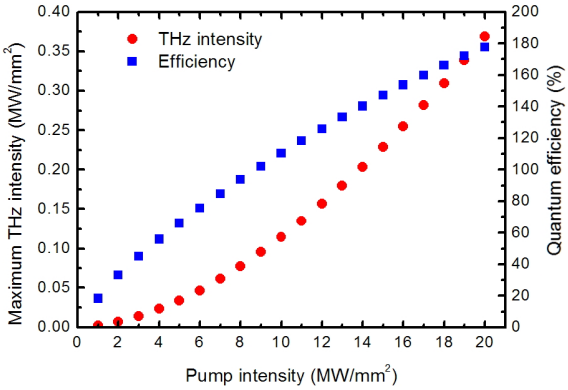

FIG. 6. The maximum THz intensity and quantum conversion efficiency versus pump intensity. Assuming pump and signal frequencies are 193.55 and 192.55 THz, respectively.

efficiency in a cascaded DFG processes. The maximum THz intensity and quantum conversion efficiency are calculated when the original pump intensities are changed from 1 MW/mm^2 to 20 MW/mm^2, as shown in Fig. 6. In the calculations, pump wave and signal wave are supposed to be 193.55 and 192.55 THz, respectively. Fig. 6 demonstrates that the maximum THz intensity and quantum conversion efficiency significantly increase with the pump intensity. THz wave with a maximum intensity of 0.3686 MW/mm^2 can be generated as pump intensity equals to 20 MW/mm^2, corresponding to the quantum conversion efficiency of 177.9%. The quantum conversion efficiency of 177.9% in cascaded processes exceeds the Manley-Rowe limit.

THz generation with the frequency of 1 THz with a collinear modal phase-matching scheme based on cascaded DFG processes is theoretically analyzed above. As for THz waves with frequencies lower than 1 THz, THz generation can be effectively enhanced based on cascaded DFG processes if the collinear modal phase-matching scheme is satisfied. As for THz waves with frequencies larger than several THz, the output of the THz wave is seriously affected by

the absorption by the GaP crystal as the absorption coefficients of THz wave in GaP crystal rapidly increase with the increase of frequency.

IV. CONCLUSION

THz generation by GaP ridge waveguide with a collinear modal phase-matching scheme based on cascaded DFG processes is theoretically analyzed. The cascaded DFG processes comprise the Stokes interaction processes and the cascaded anti-Stokes interaction processes. The calculation results indicate that the Stokes processes are stronger than the anti-Stokes processes. Compared with non-cascaded DFG processes, THz intensities from 11-order cascaded DFG processes are increased to 5.48. THz wave with a maximum intensity of 0.3686 MW/mm^2 can be generated as pump intensity is 20 MW/mm^2, corresponding to the quantum conversion efficiency of 177.9%. The quantum conversion efficiency of 177.9% exceeds the Manley-Rowe limit, providing us an efficient way to enhance the output of THz waves.

ACKNOWLEDGMENT

This work was supported by the National Natural Science Foundation of China (Grant Nos. 61201101 and 61205003) and Young Backbone Teachers in University of Henan Province (Grant No. 2014GGJS-065).

REFERENCES

1. S. Koenig, D. Lopez-Diaz, J. Antes, F. Boes, R. Henneberger, A. Leuther, A. Tessmann, R. Schmogrow, D. Hillerkuss, R. Palmer, T. Zwick, C. Koos, W. Freude, O. Ambacher, J. Leuthold, and I. Kallfass, "Wireless sub-THz communication system with high data rate," Nature Photon. **7**, 977-981 (2013).
2. C. M. Watts, D. Shrekenhamer, J. Montoya, G. Lipworth, J. Hunt, T. Sleasman, S. Krishna, D. R. Smith, and W. J. Padilla, "Terahertz compressive imaging with metamaterial spatial light modulators," Nature Photon. **8**, 605-609 (2014).
3. M. Johnston, "Plasmonics: Superfocusing of terahertz waves," Nature Photon. **1**, 14-15 (2007).
4. M. Tonouchi, "Cutting-edge terahertz technology," Nature Photon. **1**, 97-105 (2007).
5. R. Köhler, A. Tredicucci, F. Beltram, H. E. Beere, E. H. Linfield, A. G. Davies, D. A. Ritchie, R. C. Iotti, and F. Rossi, "Terahertz semiconductor-heterostructure laser," Nature **417**, 156-159 (2002).
6. K. L. Yeh, M. C. Hoffmann, J. Hebling, and K. A. Nelson, "Generation of 10 μJ ultrashort terahertz pulses by optical rectification," Appl. Phys. Lett. **90**, 171121 (2007).
7. B. S. Williams, "Terahertz quantum-cascade lasers," Nature Photon. **1**, 517-525 (2007).
8. G. L. Carr, M. C. Martin, W. R. McKinney, K. Jordan, G. R. Neil, and G. P. Williams, "High-power terahertz radiation from relativistic electrons," Nature **420**, 153-156 (2002).
9. Y. J. Ding, "Quasi-single-cycle terahertz pulses based on broadband-phase-matched difference-frequency generation in second-order nonlinear medium: high output powers and conversion efficiencies," IEEE J. Select. Topics Quantum Electron. **10**, 1171-1179 (2004).
10. W. Knap, J. Lusakowski, T. Parenty, S. Bollaert, A. Cappy, V. V. Popov, and M. S. Shur, "Terahertz emission by plasma waves in 60 nm gate high electron mobility transistors," Appl. Phys. Lett. **84**, 2331-2333 (2004).
11. Y. J. Ding, "Progress in terahertz sources based on difference-frequency generation," J. Opt. Soc. Am. B **31**, 2696-2711 (2014).
12. A. Majkić, M. Zgonik, A. Petelin, M. Jazbinšek, B. Ruiz, C. Medrano, and P. Günter, "Terahertz source at 9.4 THz based on a dual-wavelength infrared laser and quasi-phase matching in organic crystals OH1," Appl. Phys. Lett. **105**, 141115 (2014).
13. B. Dolasinski, P. E. Powers, J. W. Haus, and A. Cooney, "Tunable narrow band difference frequency THz wave generation in DAST via dual seed PPLN OPG," Opt. Express **23**, 3669-3680 (2015).
14. K. Saito, T. Tanabe, and Y. Oyama, "Design of a GaP/Si composite waveguide for CW terahertz wave generation via difference frequency mixing," Appl. Opt. **53**, 3587-3592 (2014).
15. P. Liu, D. Xu, H. Yu, H. Zhang, Z. Li, K. Zhong, Y. Wang, and J. Yao, "Coupled-mode theory for Cherenkov-type guided-wave terahertz generation via cascaded difference frequency generation," IEEE J. Lightwave Technol. **31**, 2508-2514 (2013).
16. A. J. Lee and H. M. Pask, "Cascaded stimulated polariton scattering in a Mg:$LiNbO_3$ terahertz laser," Opt. Express **23**, 8687-8698 (2015).
17. K. Saito, T. Tanabe, and Y. Oyama, "Cascaded terahertz-wave generation efficiency in excess of the Manley-Rowe limit using a cavity phase-matched optical parametric oscillator," J. Opt. Soc. Am. B **32**, 617-621 (2015).
18. K. Saito, T. Tanabe, Y. Oyama, K. Suto, and J. Nishizawa, "Terahertz-wave generation by GaP rib waveguides via collinear phase-matched difference-frequency mixing of near- infrared lasers," J. Appl. Phys. **105**, 063102-1~063102-2 (2009).
19. I. Shoji, T. Kondo, A. Kitamoto, M. Shirane, and R. Ito, "Absolute scale of second-order nonlinear-optical coefficients," J. Opt. Soc. Am. B **14**, 2268-2294 (1997).
20. T. D. Wang, Y. C. Huang, M. Y. Chuang, Y. H. Lin, C. H. Lee, Y. Y. Lin, F. Y. Lin, and G. K. Kitaeva, "Long-range parametric amplification of THz wave with absorption loss exceeding parametric gain," Opt. Express **21**, 2452-2462 (2013).
21. J. Xia, J. Yu, Y. Li, and S. Chen, "Single-mode condition for silicon rib waveguides with large cross sections," Opt. Eng. **43**, 1953-1954 (2004).
22. P. Yeh and A. Yariv, *Photonics: Optical Electronics in Modern Communication* (Oxford University Press, New Delhi, 2007).
23. M. Bass, J. M. Enoch, E. W. Van Stryland, and W. L. Wolfe, *Handbook of Optics*, 2nd ed. (McGraw-Hill, New York, USA, 2001).
24. E. D. Palik, *Handbook of Optical Constants of Solids* (Academic Press, San Diego, USA, 1998).
25. T. Tanabe, K. Suto, J. Nishizawa, K. Saito, and T. Kimura, "Tunable terahertz wave generation in the 3- to 7-THz region from GaP," Appl. Phys. Lett. **83**, 237-239 (2003).